PAPER • OPEN ACCESS

Development and verification of simultaneous measurement system for texture and phase fraction by time-of-flight neutron diffraction at iMATERIA

View the article online for updates and enhancements.

Development and verification of simultaneous measurement system for texture and phase fraction by time-of-flight neutron diffraction at iMATERIA

Y Onuki[1]**, A Hoshikawa**[1]**, S Sato**[1,2]**, S Nishino**[1,2]**, T Ishigaki**[1] **and T Tomida**[3]

[1] Frontier Research Center for Applied Atomic Sciences, Ibaraki University, 162-1 Shirakata, Tokai, Ibaraki 319-1106, Japan.
[2] Graduate School of Science and Engineering, Ibaraki University, 4-12-1 Nakanarusawa, Hitachi, Ibaraki 316-8511, Japan.
[3] Ibaraki Prefectural Government, 162-1 Shirakata, Tokai, Ibaraki 319-1106, Japan.

yusuke.onuki.0@vc.ibaraki.ac.jp

Abstract. The authors have developed the simultaneous measurement scheme for texture and phase fraction by using the Time-Of-Flight (TOF) neutron diffractometer, iMATERIA at J-PARC MLF, Japan. The Rietveld texture analysis (RTA) was applied for the data analysis method, which has been developed mainly at HIPPO diffractometer at LANSCE, USA. Because of the differences of measurement scheme and machine specifications, the analysis for the data from iMATERIA requires some special treatments. In this paper, we provide instructional information for the measurement at iMATERIA and subsequent RTA to determine the textures and phase fraction in metallic materials. The instrumental features and measurement procedures are firstly introduced. Second, some unique data treatments, especially about the technique called "scale factor bounding" is explained, including how to set it. We also suggest some refinement strategies especially aiming to have accurate phase fraction determination.

1. Introduction

The textures and phase fractions in metallic materials are key features of the microstructure to control the performances. As discussed in many papers, consideration of texture is necessary to determine phase fractions accurately by diffraction techniques [1-3]. As reported in the previous papers, the authors have developed the measurement scheme of texture and phase fraction in steels by using time-of-flight (TOF) type neutron diffractometer, iMATERIA at J-PARC MLF, Japan [4-7]. By acquiring multiple diffractograms (TOF-intensity relationships) corresponding to various sample directions, Rietveld texture analysis (RTA) can simultaneously refine ODF, *i.e.*, texture, and various phase parameters including the volume fraction of each phase.

The RTA based on TOF neutron diffraction data was firstly proposed by Wenk *et al.* [8] and extensively utilized at HIPPO diffractometer at LANSCE, USA [9,10]. The data importing, and subsequent RTA can be conducted by using MAUD software, which has been developed by Lutterotti [11,12].

Although the Rietveld analysis is a computational approach, it does not "automatically" give users an appropriate result in all cases. Users should understand the procedures, have a strategy of refinement, and carefully review the result [13].

There are many practical instructions and examples for analysis using MAUD based on data measured at HIPPO [9,10]. Also in case of iMATERIA, most of those can be applied in the same manner. However, users may need some specific features and strategies for the data measured by iMATERIA because of the characteristics of instrument and measurement scheme. Additionally, the techniques at iMATERIA focus on the application for metallic materials used in industry while most of instructive literatures for HIPPO showed examples of minerals. The authors' previous papers somewhat focused on the verifications of the measurement and analysis but limited information was provided about the detailed procedures. In this paper, therefore, we introduce some features of iMATERIA and practical procedures of RTA by using MAUD to determine textures and phase fractions in metallic materials.

2. Instrumental features
2.1. Fundamental specifications of iMATERIA
iMATERIA locates at 20th beamline at J-PARC MLF, Japan. It accepts the pulse neutron beam from the poisoned moderator [6,7], resulting in an ideal balance between intensity and resolution. Numerous detectors are equipped around the incident beam axis as shown in figure 1, which enables the simultaneous detection at various 2θ. The names of "Banks", groups of the detectors, in figure 1 indicate approximate 2θ angles in degree. Although iMATERIA has more detectors below $2\theta = 30°$ and small angle neutron scattering (SANS) bank, they are not used in the current purpose. The detectors consist of the arrays of position-sensitive tube detectors (1D-PSDs). Hence, it is possible to set arbitrary positions and areas on the detectors as the independent 0D detectors. We call them "observation points" (OPs). As shown in figure 1, we set 132 OPs (small rectangles). Each OP acquires a diffractogram corresponding to different scattering vector direction. Further details *e.g.* the geometrical distribution of OPs, can be found in the previous papers [4].
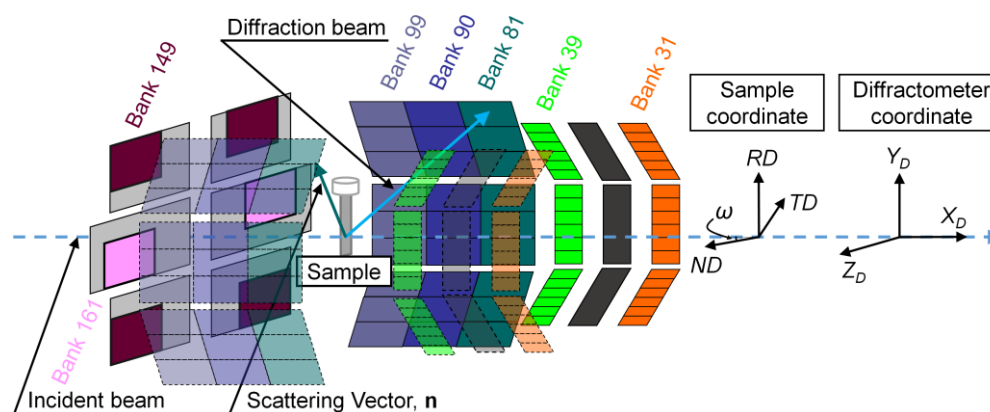

Figure 1. Schematic drawing of iMATERIA.

2.2. Sample Setting
Currently, 4 types of sample holders shown in figure 2 are available for the measurement in ambient environment. The sheet holder (figure 2 (a)) is mainly used for the samples from the industry. The standard length and width of the sample are 65 mm and 8 mm, respectively. There should be a hole for a screw pin. The diameter of the hole is 2.5 mm and the center of the hole is 5 mm away from the top end. It can hold the sample thickness up to 6 mm. Thin sheets are usually laminated so that the total thickness becomes 6 mm.

The cylindrical vanadium cells (figure 2 (b) and (c)) are used for smaller test pieces. Since the coherent scattering length of vanadium is very small, the diffraction from the cell is negligibly weak [14]. Therefore, vanadium is frequently used as the "transparent" material for various neutron diffraction

experiments. In order to fix a small sample inside the cell, polyimide films are attached both on top and bottom of the sample as shown in figure 2 (e). These prevent the sample tilt or rotate during the transfer to the measurement position.

For the samples which cannot be inserted into the cells, the cramp holder shown in figure 2 (d) is applied. In the photograph, a quartz single crystal (approximately 15 mm×10 mm×10 mm) is put between the cut pieces of vanadium cells. Because of the side pillars (white bars in the photograph), available sample angle (ω in figure 1) is limited. However, the pillars do not shut the paths of neutron beams at all when ω is set at around 30°. Use of glue to hang the sample is discouraged at iMATERIA because it is often embrittled in vacuum and the sample falls from the height of around 1.5 m to the bottom of sample chamber.

All the sample holders are attached to the white plastic (polyoxymethylene) caps seen in figure 2 (a ~ c), which are held by the sample changer [15]. The cap has a radio-frequency identification (RFID) chip which records an individual sample ID number for the measurement/storage management. The sample changer can introduce ω rotation and vertical movement along Y_D. Therefore, the beam spot position can be adjusted by moving the sample if necessary. The beam spot size is also adjustable by changing the size of the incident beam slit. The squares shown in figure 2 indicate the typical spot sizes (20 mm × 20 mm or 15 mm × 15 mm) and positions.
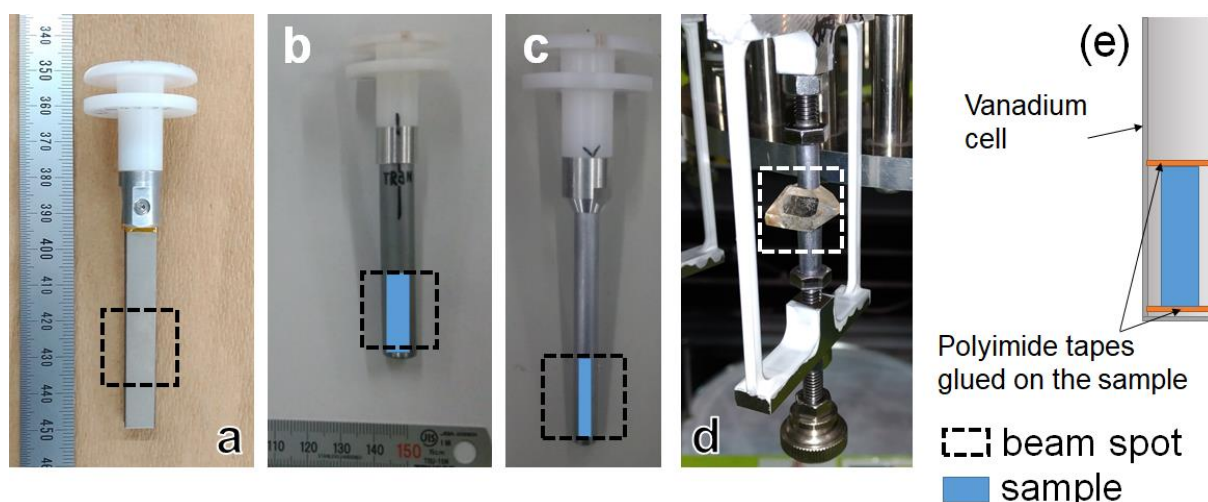

Figure 2. Sample holders used at iMATERIA. (a) sheet sample (65 mm × 8 mm) holder, (b) ϕ9.8 mm (inner diameter) cylindrical cell made of vanadium, ϕ5.8 mm vanadium cell, (d) cramp holder for irregular shape, and (e) schematic for the sample fixing in the vanadium cell.

2.3. Neutron diffraction measurement

The neutron pulse at J-PARC MLF is generated from the proton beam with the frequency of 25 Hz. For most of the metallic crystals, iMATERIA accepts every pulse (single frame mode). This results in the maximum d of approximately 0.25 nm for the backscattering banks (Banks 161 and 149 in figure 1), 0.35 nm for the side banks (Banks 99-81) and 0.9 nm for the low angle banks (Banks 39 and 31). By limiting the accepting frequency to 12.5 Hz (double frame mode), the maximum d becomes double but the scattering intensity per unit time becomes half. The double frame mode is advantageous for materials having large unit cells, *e.g.*, natural rocks and intermetallics [6].

The time for the measurement depends on the coherent scattering cross section, σ_c of the elements, the sample volume, and the proton beam power at J-PARC. In case of a steel sample held by the sheet holder, satisfactory data could be acquired in 5 minutes with the single frame mode when the proton beam power was 150 kW. The beam power is currently increasing, and it will reach to 1 MW in close future. It is confirmed that the incident neutron flux proportionally increases with the proton beam power. Therefore, the measurement time will become much shorter in future.

3. Analysis

3.1. Data format and importing

Since MAUD accepts the input data described in the format of GSAS, another Rietveld solver, details of the data format can be found in the GSAS manual [16]. Although there are several types of the input data formats, we use the "ESD" format and give the extension "gda". In the following, this type of data file is called a "GDA file". The other files are also referred by capitalized extensions. The appearance of a GDA file in the text editor is shown in figure 3. In this format, the intensity and its expected standard deviation are alternatively described with a constant binning width of TOF (usually 8 μs is applied for cubic and HCP metals). It should be noted that the values of intensity and standard deviation recorded in this file are not "raw" measured data but results of external normalization by the incident beam intensity [14]. Although MAUD/GSAS can deal with the incident spectrum as a continuous function, the incident spectrum profile at iMATERIA is too complex to be represented by the prepared functions.

The GDA file includes the 132 datasets (diffractograms) corresponding to the OPs. The sequential numbers are distributed as BANK 1, BANK 2, …, BANK 132. It should be noted that the terminology, "BANK" used here actually corresponds to the OP, a part of the detector. In this paper, we use "Bank" for the group of OPs having similar 2θ, as indicated in figure 1.

There is also a file describing the instrumental parameters of the 132 OPs (*.PRM). This file describes the positions of the OPs and instrumental profile functions describing the standard shapes of diffraction peaks. In addition, the conversion parameters, DIFC, DIFA, ZERO are also recorded. These parameters are used to convert TOF to d spacing in angstrom. These instrumental parameters are basically dealt as the constant (fixed) values in the following analysis. Therefore, regardless of the sample, the same PRM file can always be used. Strictly speaking, DIFC is often the value to be refined in multi-diffractogram analysis because this can be affected by the sample shape, kind of element and sample density [9]. However, the refinement of DIFC is usually very fine tuning, which makes the variation less than 1 percent of the value.

The "HIPPO wizard" can be used to import the GDA and PRM files (even though the instrument is not HIPPO but iMATERIA!). The sample setting angle ω is also asked in the dialog. After the data import, the whole parameters can be saved as the analysis file (*.PAR file). Subsequently, phase initial parameters are prepared. Since the crystal structures of metals are very simple, it may be possible to set them manually. However, it is easier to import CIF or MDB file. The former is written in the universal format [17] to describe the crystal structure of a certain phase. The latter is a set of CIF files. You may find "structures.mdb" in the MAUD directory and chose what you need to include from numerous phase data. The MDB files can be created by simply copy and paste the multiple CIF data into a single file. It is convenient to have one's own MDB library including only the phase data which you frequently refer to.
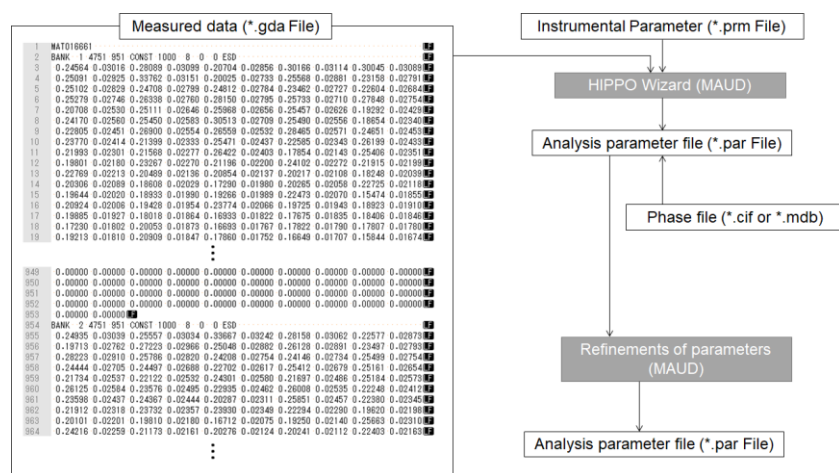

Figure 3 the input files to start the Rietveld texture analysis using MAUD.

3.2. Characteristic settings for iMATERIA

3.2.1. Bank grouping Tolerance. In order to have the Bank groups shown in figure 1, firstly, the tolerance angle of 2θ for the Bank grouping must be changed to 6°. By selecting "Analysis > Preferences" at the top menu bar, a table of values become visible. In this list, you can find "hippoWizard.maxDelta2ThetaForBankGrouping" and set the value as "6". Then click "save on disk", and "OK" to close the table, and restart MAUD. This is not mandatory, but the appropriate bank grouping makes the comparison between measured and computed diffractograms easier, especially in the 2D plotting. This should be done before starting "HIPPO wizard" and creating the PAR file.

3.2.2. Scale factor bounding. After creating the PAR file (either before or after importing phase information), we introduce the "scale factor bounding", which forces the scale factors belonging to the same Bank group to have the same value. The scale factor is the value to adjust the overall height of the computed diffractogram. This is basically a meaningless value but one of the most important values to have a good agreement between the computed and measured diffractograms.

When the authors developed the texture measurement scheme with only one neutron exposure, we encountered the problem that the scale factors belonging to the same Bank group varied in a certain range, resulting in inferior fitting. On the other hand, the scale factors in the same Bank group converged into an almost identical value for non-textured powder materials and a good fitting quality was obtained. The latter seemed to be more appropriate because the intensity normalization described above should compensate the differences of detecting efficiencies among the OPs. Therefore, we introduced the scale factor bounding, which improved the result and stability of the analysis for textured materials.

The scale factor variation that we observed was probably because that one OP measures only one diffractogram at iMATERIA. When we use 3~5 GDA files measured at different ω angles (as HIPPO does), the variation of the scale factors was suppressed. Since one OP measures multiple diffractograms for different sample directions in this case, the scale factor for this OP should be chosen to fit all the diffractogram. In other words, the effect of texture on the scale factor is somewhat cancelled or averaged. On the other hand, when one OP measures just one diffractogram, there arises the ambiguity; which should be applied to explain the diffractogram having large peaks, high pole densities or large scale factor?

When the scale factor bounding is introduced, a unique scale factor is determined by considering all the diffractograms belonging to the Bank group. As the complementary effect, this increases the calculation speed due to the reduction of parameters to be refined.

The scale factor bounding can be introduced by changing the refinement status of the scale factors. One of them in a certain Bank group needs to be "refined" but the others are set "equal to" the refined one. Since there are 132 scale factors and 7 Bank groups, 125 statuses of scale factors should be changed. Because it is very time-consuming to do this procedure manually on MAUD GUI, we developed a simple software to modify the PAR file so that the above procedure is conducted in a moment.
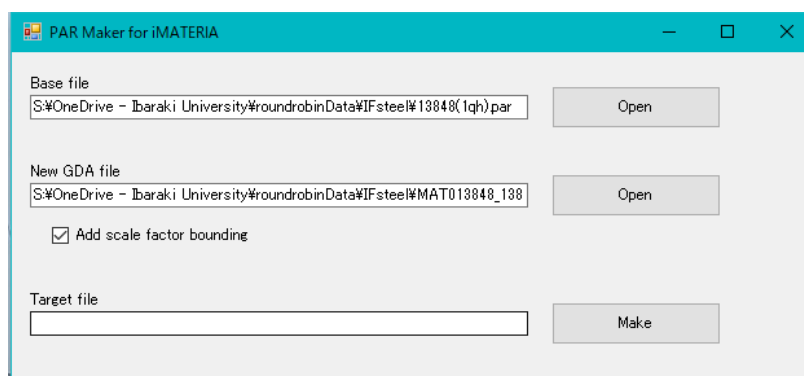

Figure 4. Screenshot of the "PAR Maker", which applies the scale factor bounding and/or makes a clone PAR file.

The screenshot of this software is shown in figure 4. This software can also be used to create a "clone" PAR file, which has the same parameters as the base but GDA file data is replaced. When the replacement of measured data is not needed, a user chooses the PAR file made by HIPPO wizard, specify the GDA file which was chosen in the wizard, and check the "Add scale factor bounding". Finally, by clicking "Make", the new PAR file with the scale factor bounding is created. The file name can be specified by the save-file dialog. The textbox of "Target file" shows the full-path name of the new PAR file after the job is completed.

By specifying different GDA file from that included in the base PAR file, the data is replaced by the new GDA file, *i.e.,* another measurement. This is useful to analyse the series of samples having similar conditions. It is unnecessary to repeat HIPPO wizard and set phases for every sample if a user uses this software. However, one should pay attention that this process may introduce a certain bias on the analysis. We recommend resetting ODF for every phase in the clone PAR file at the start of refinement. Based on our experience, the ODF calculation converges faster by stating from a random ODF than a certain "wrong" texture.

3.3. Refinement

3.3.1. General settings. Before starting the refinement, several settings are required. The detailed procedures can be found elsewhere [9]. In this paper, we simply introduce what we apply. We recommend using MAUD version 2.7.1 or higher.

As the ODF calculation method, E-WIMV method [11] is applied. The ODF resolution of 5° works the best for most of structural metallic materials. The default sample coordinate is fixed at the diffractometer coordinate, X_D-Y_D-Z_D, in MAUD. Therefore, artificial rotation of the sample is necessary so that X_D, Y_D, and Z_D respectively correspond to the RD, TD, and ND in case of the rolled sheet. figure 5 shows the values of rotation angles for the rolled sheet with three typical setting geometries.
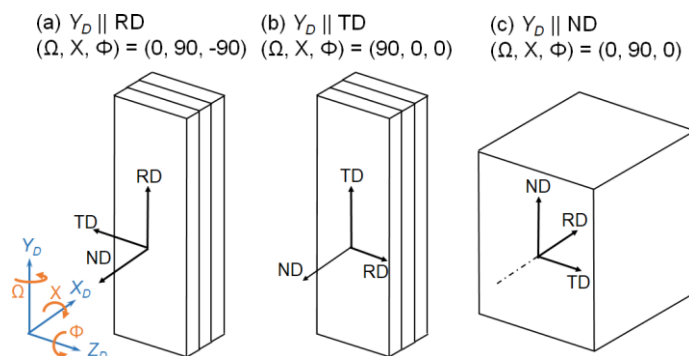

Figure 5. Sample rotations to fit the RD-TD-ND coordinate to the diffractometer coordinate,

3.3.2. Automatic refinement wizard. In the Rietveld analysis, a user can "refine" (deal as variables) almost all the parameters at the same time. However, having too many variables at the beginning quite often results in divergence, *i.e.* the calculated fitting curve goes far away from the measured diffractogram. Therefore, one needs to have a "strategy of refinement"; what should be fixed or to be refined at first, and what to do after that? The automatic refinement wizard provides some sets of the refinement strategies. In case of textured metallic materials, one can use "Texture analysis" in the wizard. This automated refinement process automatically conducts the refinements in the following four steps.

i.   background (BG) and scale factor (SF).
ii. lattice parameter (only *a* for cubic phases), DIFC, Debye-Waller factors (B_{iso}) + BG and SF.
iii. Microstrain (ε) and crystallite size (D) + BG, SF, *a*, DIFC, B_{iso}.
iv. Mutual refinement of ODF and Rietveld parameters: ε, D, a, DIFC, B_{iso}, BG, SF.

At each step, several cycles of iterative calculation are conducted. We recommend conducting 4 cycles. Applying too few cycles may result in divergence.

If the main purpose of the analysis is the texture analysis of a single-phase steel, a satisfactory result can be achieved only by doing this. However, in some cases, additional iteration with more parameters are necessary as described below.

3.3.3. Individual refinement of Debye-Waller factor for each phase. The Debye-Waller factor, B_{iso}, also called the temperature factor, represents the effect of the thermal vibration of the atoms on the diffractogram. This introduces the gradual decrease of the diffraction intensities with decreasing d (or increasing Q, technically) [18]. By conducting the above automatic refinement, the Debye-Waller factors, B_{iso} for all the phases are bound in to one value. This is a good assumption at the initial stage not to reach divergence. However, For the accurate determination of the phase fraction, B_{iso} for each phase should be separately refined. The separate refinement can simply be done by changing the refinement status from "equal to" to "refine", and a few cycles of refinement. With decreasing B_{iso}, the overall diffraction intensity increases. Therefore, underestimation of B_{iso} causes the underestimation of the phase fraction.

Table 1 shows examples of analyses with separated and bounded B_{iso} refinement for the laminated steel sample used in the previous study [4]. The FCC (austenite) phase tends to have larger Biso than that of BCC (ferrite) phase. When B_{iso} for both phases are bounded into one value, the phase fraction of austenite is underestimated, as expected above. Peng et al. reported that B_{iso} for BCC and FCC iron at 293 K were 0.3250 and 0.5577, respectively [18]. Although the values for alloy steels can be different, it is always important to check if the value of B_{iso} is around these values. Sometimes, a negative value or extremely large value (>1) is obtained. In such case, some other parameters (most likely texture) are wrongly determined, or an absorption model should be considered.

To take the absorption into account, "Harmonic Coeff." sample shape model works very well. The sample symmetry should be "*2/mmm*" for rectangular samples. "*Cylinder*" symmetry is also used for cylindrical bars and wires. Since both the absorption and thermal vibration bring gradual change of scattering intensity depending on d, they seem to affect each other in the refinement. Based on our experiences, the steels containing Mn or Co often require the consideration of absorption while there seems to be negligible absorption for low carbon steels and Si steels.

When the fraction of the secondary phase is a few percent or smaller, the refinement of B_{iso} tends to be very unstable. In such case, it is better to have a fixed value, according to the table provided by Peng *et al.*, rather than applying an unreliable refined value.

Table 1. Refinement conditions and resulted values of Debye-Waller factors and Austenite fractions in the laminated SUS430-SUS316L composite sample. The prepared fraction of austenite was 19.4 vol%.

B_{iso} refinement	Separate	Bounded
B_{iso} (ferrite)	0.27	0.25
B_{iso} (austenite)	0.48	0.25
Austenite fraction (vol %)	19.1	17.4

3.3.4. Chemical composition. In most multiphase materials, each phase has a different chemical composition even if it is a solid solution. As the neutron scattering intensity depends on the elements, the chemical compositions should be considered for the accurate phase fraction determination. In the previous paper [4], we have reported a verification using composite samples consisting of SUS 316L austenitic stainless steel (Fe-18Cr-12Ni-1Mo, mol %) and SUS430 ferritic stainless steel (Fe-18Cr). At the beginning of the study, we obtained smaller analysed fractions of austenite than the prepared fractions in all the samples because both FCC and BCC phases were set as "pure Fe". Since SUS 316L contains a certain amount of Ni, the average scattering length was larger than that of SUS 430. By setting

alloy elements (as the atoms partially occupies the Fe site), we have reached the satisfactory results reported in that paper. If possible, one should estimate the chemical compositions of the phases by the thermodynamic calculation or measure them by EDS, which is beneficial to obtain more accurate phase fraction. Especially the effect of chemical composition would be more critical when the sample contains high amount of Ti and/or V. Since they have negative values of coherent scattering lengths, the average scattering length can largely change by adding them.

4. Summary

The simultaneous measurement system for texture and phase fraction was developed at the TOF neutron diffractometer, iMATERIA at J-PARC MLF, Japan. Most of technical backgrounds and procedures of measurement/analysis at iMATERIA are common with the pioneer, HIPPO at LANSCE, USA. However, some specific considerations and procedures are required due to the machine specification and characteristics of the measurement. Especially, the scale factor bounding, and separate Debye-Waller factor refinement are keys to obtain accurate textures and phase fractions. In some cases, consideration of the absorption relating to the sample shape and/or chemical composition must be carefully considered, which depends the elements consisting the materials.

References

[1]   Xu P G, Tomata Y, Arakaki Y, Harjo S and Sueyoshi H 2017 *Mater. Charact.* **127** 104
[2]   Jacques P J et al. (14 more autors) 2009 *Mater. Sci. Tech*. **25** 567
[3]   Scarlett N V Y, Madsen I C, Cranswick L M D, Lwin T, Groleau E, Stephenson G, Aylmoree M, and Agron-Olshina N 2002 *J Appl. Cryst.* **35** 383.
[4]   Onuki Y, Hoshikawa A,Sato S, Ishigaki T and Tomida T 2017 J. Mater. Sci. **52** 11643
[5]   Onuki Y, Hoshikawa A, Sato S, Xu P G, Ishigaki T, Saito Y, Todoroki H and Hayashi M 2016 *J. Appl. Cryst.* **49** 1579
[6]   Ishigaki T et al. (16 more authors) 2009 *Nucl. Instrum. Methods Phys. Res. A* **600** 189
[7]   Nakajima K et al (63 more authors) 2017 *Quantum Beam Sci.* **1** 9
[8]   Wenk H R, Matthies S and Lutterotti L 1994 *Mater. Sci. Forum* **157-162** 473
[9]   Vogel S C, Hartig C, Lutterotti L, Von Dreele R B, Wenk H R and Williams D J 2004 *Adv. X-Ray Anal.* **47** 431
[10] Wenk H R, Lutterotti L and Vogel S C 2010 *Powder Diffr.* **25** 283
[11] Lutterotti L, Matthies S, Wenk H R, Schultz A S and Richardson Jr J W 1997 *J. Appl. Phys.* **81** 594
[12] Lutterotti L, Chateigner D, Ferrari S and Ricote J 2004 *Thin Solid Films* **450** 34
[13] Toby B H 2006 *Powder Diffr.* **21** 67
[14] Izumi F, Asano H, Murata H and Watanabe N 1987 *J. Appl Cryst.* **20** 411
[15] Hoshikawa A et al. (14 more authors) 2009 *Nucl. Inst. Methods Phys. Res. A* **600** 203
[16] Larson A C and Von Dreele R B, 2004 *Los Alamos National Laboratory Report LAUR* 86-748
[17] Hall S R, Allen F H and Brown I D 1991 *Acta Cryst. A* **47** 655
[18] Peng L M, Ren G, Dudarev S L and Whelan M J 1996 *Acta Cryst. A* **52** 456